

## DIATOMIC DICATIONS CONTAINING ONE INERT GAS ATOM

P. JONATHAN, R.K. BOYD<sup>1</sup>, A.G. BRENTON and J.H. BEYNON

Royal Society Research Unit, University College of Swansea Singleton Park, Swansea SA2 8PP, UK

Received 4 July 1986

Diatomic dications  $AY^{2+}$ , where  $A = \text{Ne, Ar, Kr or Xe}$  and  $Y = \text{C, N or O}$ , have been detected and characterised via appearance energies, ionization energies of the corresponding monocations determined by charge-stripping, and values of translational energy release accompanying unimolecular dissociation of  $AY^{2+}$  on the microsecond timescale. The mechanism of formation of  $AY^{2+}$  is unclear, but possibly involves three-body association of  $A^{2+}$  and  $Y$ . Approximate potential curves for some of these dications have been generated using the semi-empirical procedure due to Hurley, and applied in a general interpretation of some of the trends observed.

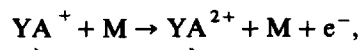
### 1. Introduction

A theoretical investigation [1], at the self-consistent field level, of cations containing a helium atom led to the prediction that diatomic dications comprised of an inert-gas atom plus an atom of a first-row element should be stable. The present work is devoted to an experimental investigation of such species, together with semi-empirical calculations of some potential curves based upon the method due to Hurley [2,3].

Recently [4] we reported the results of an experimental investigation of monocations formed from inert gas atoms plus other atoms or small molecules or radicals. This work [4] included a review of current knowledge of such cations, which need not be repeated here. Experimental and theoretical knowledge concerning dications containing inert-gas atoms is much more sparse. To our knowledge the only experimental evidence for such species are an observation [5] of  $\text{XeNe}^{2+}$  formed in the three-body association reaction  $\text{Xe}^{2+} + 2\text{Ne} \rightarrow \text{XeNe}^{2+} + \text{Ne}$ , measurements of appearance energies [6,7] of  $\text{XeNe}^{2+}$ ,  $\text{XeAr}^{2+}$  and  $\text{KrNe}^{2+}$  from the corresponding mixed van der Waals di-

mers, and detection [8] of  $\text{He}_2^{2+}$  formed by charge-stripping of  $\text{He}_2^+$ .

The present work grew out of a reinvestigation [4] of the classic work of Field and Franklin and their collaborators [9-12] on monocations of the type  $YA^+$ , where  $A$  represents an inert-gas atom and  $Y$  is an atom, small molecule or radical. Attempts were made [4] to observe stable dications  $YA^{2+}$ , formed by charge-stripping processes



where  $X$  denotes a species  $X$  with laboratory-frame translational energies in the keV range. In all cases where  $Y$  was a polyatomic species (e.g.  $\text{CH}_4$ ,  $\text{NH}_3$ ,  $\text{O}_2$  or  $\text{N}_2$  [4]) no  $YA^{2+}$  products could be detected after the few microseconds appropriate to the experimental technique used, although some evidence was obtained for singly charged fragments which had arisen from unstable  $YA^{2+}$ . However, in cases where  $Y = \text{C, N or O}$ , many of the resulting  $YA^{2+}$  species could be detected, and it is these unusual species which are described here.

### 2. Experimental

The experiments reported here were conducted using a VG Analytical ZAB-2F double-focusing

<sup>1</sup> Present address: Department of Chemistry and Biochemistry, University of Guelph, Guelph, Ontario, Canada N1G 2W1

mass spectrometer of reversed configuration (magnet preceding electric sector) which has been described previously [13]. Addition of a second electric sector [14] permits identification and removal of artifacts of various kinds [15] in mass-analysed ion kinetic energy (MIKE) spectra such as those reported here. Indeed, due to the very low intensities of the  $YA^{2+}$  species relative to those of ions with higher  $m/z$  values in the present experiments, the artifacts were in many cases more intense than the signals of interest. The latter could then not have been detected if the second electric sector had not been available. All results reported here were obtained by selecting the main beam of precursor ions using the double-focusing combination and characterising the products by scanning the second electric sector [15]. The low-level signals (single-ion limit) were characterised by multiple-scan accumulation using a computer-based data system described previously [16].

The conventional Nier-type electron ionization source was operated at pressures somewhat higher than usual, but trap-stabilisation of the electron beam current could still be achieved. Gas mixtures were made up in glass bulbs, and allowed to mix thoroughly before use. In order to prepare ion beams of  $AC^+$ ,  $AN^+$  and  $AO^+$ , or of the corresponding dications, mixtures of the appropriate rare gas A were prepared in a 50% mole ratio with  $CH_4$ ,  $N_2$  and  $O_2$ , respectively. Other experimental details are given in the appropriate sections below.

### 3. Results

#### 3.1. Charge-stripping of monocations $YA^+$

The procedures used to calibrate the translational energy scale were the same as those described previously [17]. Species used in this calibration were both the inert-gas ion  $A^+$  extracted from the same ion-source from which  $YA^+$  was selected, or the molecular ion of toluene formed in a separate experiment. The two procedures yielded very similar results, within the rather large uncertainties associated with the weak signals for  $YA^{2+}$ . Fig. 1 shows a typical example. The collision gas used was nitrogen.

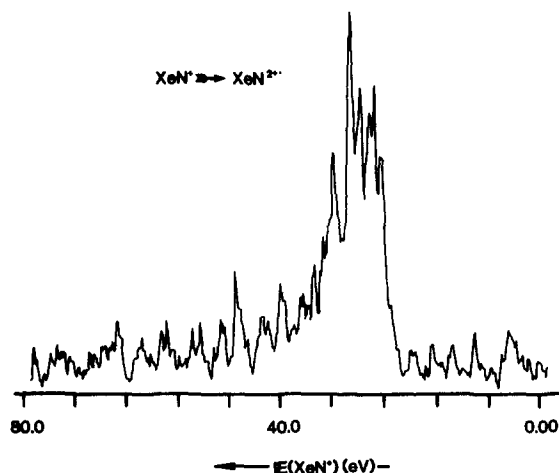


Fig. 1 Charge-stripping peak for  $XeN^+$  in collision with  $N_2$ . Accelerating potential 7 kV.

Table 1 summarises the results thus obtained. Only six of the twelve possible combinations  $YA^+$  yielded charge-stripping signals of intensity sufficient that estimates of ionization energies could be made. The experimental uncertainties quoted in table 1 are, for the same reasons, much larger than are usual ( $\pm 0.5$  eV) in work of this type [17]. The value obtained for  $XeC^+ \rightarrow XeC^{2+} + e^-$  seems unusually low, but represents the average of ten independent determinations together with five independent calibration runs. The failure to determine the ionization energy of  $ArC^+$  was particularly unfortunate in that this ion was present at reasonable intensity, but was accompanied by  $C_4H_4^+$  ions of the same nominal mass. It was possible to resolve this mass doublet, but at the cost of reducing the intensity of the desired charge-stripping signal to unusable levels.

Table 1  
Ionization energies (eV) of  $YA^+$  monocations obtained by charge-stripping experiments

	C	N	O
Xe	$16.6 \pm 1.0$	$21.1 \pm 2.2$	$19.6 \pm 2.6$
Kr	—	$21.6 \pm 1.8$	$22.5 \pm 1.4$
Ar	—	$20.7 \pm 2.5$	—
Ne	—	—	—

### 3.2. Charge-separation reactions of $YA^{2+}$ dications

It is well known that diatomic dications can undergo unimolecular dissociation on the micro-second timescale appropriate to mass spectrometers. Mechanisms for such delayed predissociation processes can involve either tunnelling from a quasi-bound level through a potential barrier, or electronic curve crossing between states of different multiplicities (spin-forbidden crossings). In either case, the predissociating level is anticipated to lie at several eV above the separated-ion limit ( $Y^+ + A^+$ ), due to the important contribution of the coulombic repulsion to the net interaction. All of this excess energy must appear as relative translational energy of the separating atomic fragments. When transformed to laboratory-fixed coordinates, this relative motion gives rise [18] to a greatly amplified spread of translational energies of the product ions. Since there is no focusing action in the direction mutually perpendicular to the main instrumental axis and to the electric field within the analysing sector (the  $z$ -direction), the product ions which have received their share of the excess energy in this direction may follow trajectories which carry them beyond the  $z$ -heights of the final slit of the apparatus. Such ions are thus lost, resulting in wide and deeply dished peaks, in the ion kinetic energy spectrum, characteristic of fragmentation reactions involving a large release of internal energy as translational energy. Charge-separation reactions are typical of this phenomenon and examples for  $YA^{2+}$ , obtained in the present work, are shown in fig. 2.

Fig. 2, which represents some of the best spectra obtained in the present work, shows how the degree of dishing of the peak, due to the  $z$ -discrimination, increases with increasing values of kinetic energy release  $T$  and decreasing mass of the detected ion. (The latter effect is important because the energy must be partitioned between the two fragments so as to conserve momentum in the centre-of-mass reference frame.) For  $NeN^{2+} \rightarrow Ne^+ + N^+$  the spectrum was extremely difficult to obtain and required high-energy (200 eV) electrons to obtain sufficient  $NeN^{2+}$  precursor ion current.

Table 2 summarises the values of  $T$  obtained in

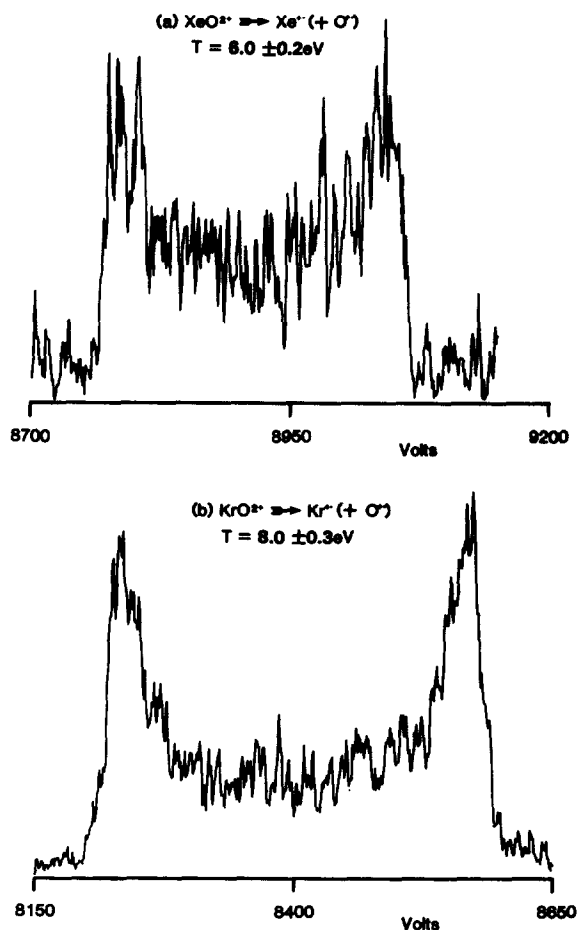


Fig. 2 Ion kinetic energy spectra for unimolecular charge-separation reactions of doubly-charged rare-gas oxides. Accelerating potential 5 kV, electron energy 100 eV. (a)  $XeO^{2+} \rightarrow Xe^+ + O^+$ ;  $T = 6.0 \pm 0.2$  eV. (b)  $KrO^{2+} \rightarrow Kr^+ + O^+$ ;  $T = 8.0 \pm 0.3$  eV.

the present work. Comparison of tables 1 and 2 shows that it is the nitrides  $AN^{2+}$  which appear to be the most stable in that they yield measurable

Table 2  
Values of translational energy release  $T$ (eV) for unimolecular charge-separation reactions of  $YA^{2+}$  dications

	C	N	O
Xe	$9 \pm 1$	$6.1 \pm 0.3$	$6.0 \pm 0.2$
Kr	—	$6.0 \pm 0.2$	$8.0 \pm 0.3$
Ar	—	—	$9.1 \pm 0.3$
Ne	—	$6.5 \pm 0.5$	—

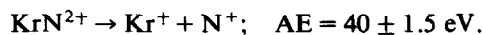
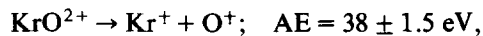
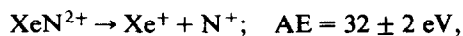
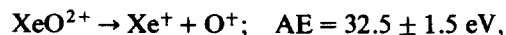
signals for both kinds of experiment. By the same criterion the carbides are the least stable.

### 3.3. Appearance energies for $AY^{2+}$ ions

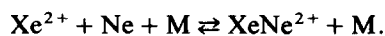
The mechanisms of formation of  $AY^{2+}$  ions, in electron impact ionization of the gas mixtures used, are likely to be chemically complex. It was hoped that measurements of appearance energies of these species might serve to restrict the range of possible mechanisms. Experimentally, it was found to be advantageous to measure appearance energies for the unimolecular charge-separation peaks (fig. 2) instead of for the  $AY^{2+}$  ions which survived the flight from ion source to detector. The latter ion currents were considerably larger, but the interferences from mass spectrometer background were sufficiently serious as to perturb, or even wholly obscure, the signals due to  $AY^{2+}$ . This was particularly true in the threshold region. This problem of "chemical noise" was completely removed for the charge-separation peaks (ion translational energies greater than that of singly charged ions in the stable main beam). In the present case this advantage outweighed the concomitant disadvantage of lower overall signal levels.

The electron energy scale was calibrated in each case by measuring ionization efficiency curves for production of the inert gas ions  $A^+$ ,  $A^{2+}$  and  $A^{3+}$  in the same experiment in which the appearance energy for the process  $AY^{2+} \rightarrow A^+ + Y^+$  was measured. In all cases studied here, the ionization efficiency curves were of a form anticipated for direct ionization processes. In particular, no evidence was obtained to suggest that metastable excited states of  $A$ ,  $A^+$  or  $A^{2+}$  were responsible for formation of  $AY^{2+}$ . Such processes are characterised [4,9–12] by sharply defined excitation functions, of which none were observed in the present work.

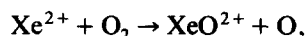
Due to the low signal levels available, these appearance energy measurements were extremely tedious, and the experimental uncertainties were large. The following values of the appearance energy (AE) were obtained:



The appearance energies for  $\text{Xe}^{2+}$  and  $\text{Kr}^{2+}$  are 33.3 and 38.6 eV, respectively. It thus appears that under the experimental conditions of the present work the mechanistic precursors of  $AY^{2+}$  ions (or at least of those which spontaneously dissociate on a microsecond timescale) are most probably the ground-state inert gas dications  $A^{2+}$ . It was shown previously [5] that  $\text{XeNe}^{2+}$  ions can be formed at pressures appreciably higher (few tenths of a Torr) than that estimated [4] to exist in the ion source in the present work ( $\approx 5 \times 10^{-3}$  Torr) via the equilibrated thermal reaction



However, for formation of  $\text{XeO}^{2+}$  ions the reaction



is probably most consistent with the measured appearance energy and that  $\text{O}_2$  is the major neutral species compared to only small concentrations of O.

## 4. Discussion

The present work represents the first report of these  $YA^{2+}$  species, and the available characteristics information is correspondingly sparse. However, it is possible to offer some rather general discussion of their properties.

The theoretical work [1], which proposed that the dications  $YA^{2+}$  might be bound more strongly than the corresponding monocations  $YA^+$ , dealt only with the case  $A = \text{He}$ . This is unfortunate, since helium is a slightly special case due to its high ionization energy (IE = 24.58 eV) which is higher than the second ionization energy (24.38 eV) of a carbon atom, for example. Thus the ground-state dissociation limits of  $\text{HeC}^{2+}$  are  $\text{C}^{2+} + \text{He}$ , rather than  $\text{C}^+ + \text{He}^+$ . In every other case of interest here the ground-state dissociation limits of  $YA^{2+}$  are indeed  $Y^+ + A^+$ , and the potential surfaces for such species might be ex-

pected to be qualitatively different from those for  $\text{HeC}^{2+}$ . The importance of this distinction was emphasised previously [6,7].

Similar considerations applied to the monocations  $\text{YA}^+$  can lead to a classification according to whether  $\text{IE}(\text{Y})$  is greater or less than  $\text{IE}(\text{A})$ . This is of some interest in view of the observation [4] that collision-induced dissociation (CID) reactions of  $\text{YA}^+$  ions, at keV energies, invariably produced the inert gas ion  $\text{A}^+$  as the major ionic product even if formation of  $\text{Y}^+$  was energetically favoured. For example, this was found to be true for  $\text{CAr}^+$ ,  $\text{NAr}^+$  and  $\text{OAr}^+$ , for which  $\text{IE}(\text{Ar})$  is greater than the IE values for C, N and O. As for all phenomena described in the present work, a proper understanding will require high-level ab initio calculations of the states of both monocations and dications. However, states of  $\text{YA}^+$  which correlate with ground-state  $\text{A} + \text{Y}^+$  can be anticipated to be essentially non-bonding, apart from a relatively weak van der Waals interaction. Excimer states [19] correlating with appropriate excited states of the inert gas atom,  $\text{A}^* + \text{Y}^+$ , might be expected to be sufficiently stable to survive to the collision region [4] but to lie at much higher energy. On the other hand, states correlating with  $\text{A}^+ + \text{Y}$  could be expected to be bound, to lie at moderate energies, and thus to dissociate to  $\text{A}^+$  ionic fragments via vibrational-rotational CID mechanisms. Of course, avoided crossings of states of the same space-spin symmetry, but correlating with different limits, could seriously affect such general considerations. However, the observation [4] that the  $\text{A}^+$  channel always dominates the CID reactions of  $\text{YA}^+$  monocations was of such wide validity that some such general discussion seems called for. These  $\text{YA}^+$  monocations are the precursors in the charge-stripping experiments reported here.

For all of the  $\text{YA}^{2+}$  dications investigated in the present experiments the ground-state dissociation limits correspond to  $\text{Y}^+ + \text{A}^+$ , rather than to  $\text{A}^{2+} + \text{Y}$ , for example. This implies that the semi-empirical procedure due to Hurley [2,3], for estimating potential curves for  $\text{YA}^{2+}$  from known curves for the isoelectronic neutral species (e.g.,  $\text{CCl}$  for  $\text{NAr}^{2+}$ ), is appropriate. Hurley's procedure [2,3] consists of superimposing a coulombic

repulsion term upon a bonding potential determined experimentally for the isoelectronic neutral species, but scaled via a procedure suggested by the virial theorem. This procedure [2,3] is known [20] to yield poor results at intermediate values of internuclear distance, where the dominant configuration correlates with the  $\text{A}^{2+} + \text{Y}$  limits (the charge-polarization states). However, the general form of the potential surfaces, and in particular the bonding regions, are often described surprisingly well by Hurley's method. Thus, it seemed worthwhile to produce such curves for  $\text{YA}^{2+}$  species of interest here.

The only problem with Hurley's procedure [2,3] involves assembling the spectroscopic information for the isoelectronic neutral species, assigning the correct dissociation limits to each of these neutral states, and determining the virial theorem scaling factor. Thereafter the procedure is straightforward. In the present work the spectroscopic information was taken from the standard critical compilation [21]. The only states considered were those (generally lower states) for which dissociation limits could be easily assigned and which were anticipated to have radiative lifetimes in the microsecond range or longer. In the original work [2,3] the scaling factor  $t$  was determined theoretically by evaluating the expectation values of the kinetic energy operator using Slater atomic functions. In the present work the value of  $t$  was estimated using a relationship given by Hurley [3]

$$\delta E_d = t^2 \Delta E_n,$$

where  $\Delta E_d$  represents specific excitation energy of the atomic dissociation products of a state of the dication, and  $\Delta E_n$  is the corresponding value for the isoelectronic neutral species. As shown by Hurley [3], this relationship is particularly appropriate for homonuclear diatomic species. For heteronuclear species one is forced to use an average of the  $t$  values determined separately for the two atomic fragments. Using excitation energies given by Moore [22], the following values for  $t$  were determined in this way:

$$\begin{aligned} &\text{C}^+/\text{B}, 1.255; \quad \text{N}^+/\text{C}, 1.227; \quad \text{O}^+/\text{N}, 1.188; \\ &\text{Ne}^+/\text{F}, 1.461; \quad \text{Ar}^+/\text{Cl}, 1.365; \quad \text{Kr}^+/\text{Br}, 1.331; \\ &\text{Xe}^+/\text{I}, 1.300. \end{aligned}$$

This procedure, while approximate, is entirely consistent with Hurley's treatment [3] of  $\text{NO}^{2+}$ . Unfortunately, no spectroscopic information is available for IB, IC or IN, so none of  $\text{XeC}^{2+}$ ,  $\text{XeN}^{2+}$  or  $\text{XeO}^{2+}$  could be treated using Hurley's procedure [2,3]. Figs. 3–5 show the results of these calculations for the species which could be thus treated.

Fig. 3 suggests that the present failure (tables 1 and 2) to obtain any evidence for the species  $\text{KrC}^{2+}$ ,  $\text{ArC}^{2+}$  and  $\text{NeC}^{2+}$  cannot be accounted for in terms of shallow or non-existent potential wells. The  $R_e$  values seem normal, so unfavourable Franck–Condon factors in the charge-stripping experiment are unlikely to explain this negative result. Possibly the ground states are predissociated by repulsive singlet states which are not located by the Hurley procedure [2,3].

The potential curve for ground-state  $\text{NeN}^{2+}$  (fig. 4) has its quasi-bound maximum at 6.1 eV above the dissociation limits. If the unimolecular dissociation, observed (fig. 2) to occur on the microsecond timescale, may be attributed to tunnelling near the top of this barrier, the experimental value of kinetic energy release (table 2) is in good agreement with this theoretical prediction.

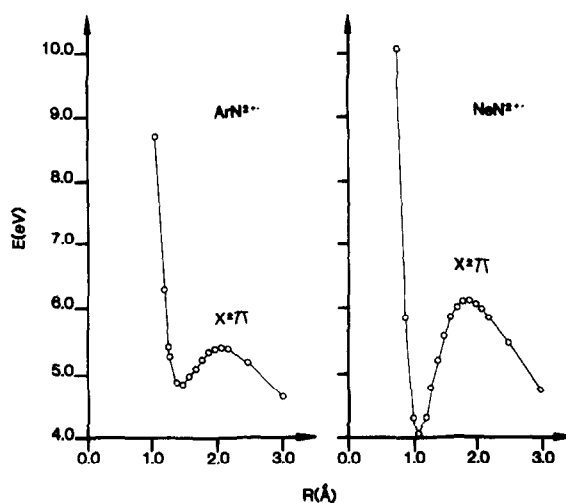


Fig. 4 Approximate potential curves for dictations of rare-gas nitrides, calculated using the procedure due to Hurley. Energy zero corresponds to ground-state atomic ion limits.

In the case of the oxides (fig. 5) the  $X^3\Sigma^-$  states arise by combination of ground-state atomic ions [ $A^+(^2P_u) + O^+(^4S_u)$ ], while the  $b^1\Sigma^+$  state must correlate with [ $A^+(^2P_u) + O^+(^2D_u)$ ] some 3.3 eV higher. Comparison of these theoretical

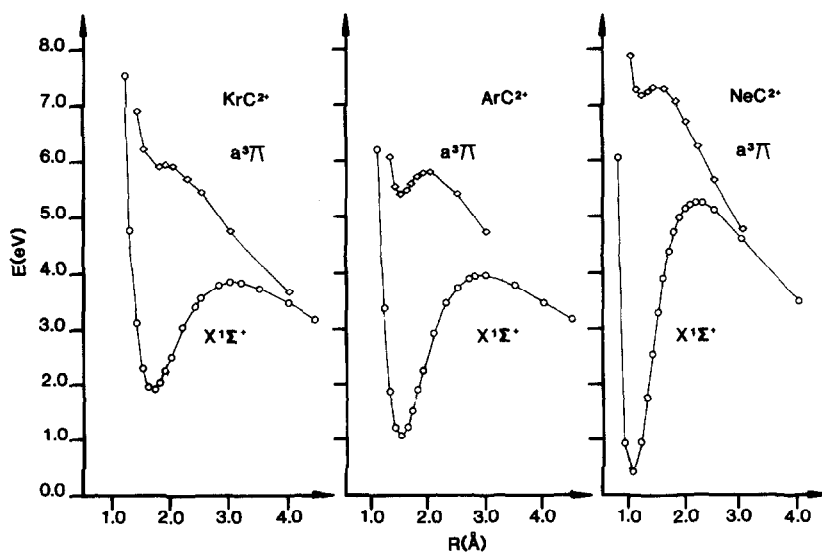


Fig. 3 Approximate potential curves for dictations of rare-gas carbides, calculated using the procedure due to Hurley. Energy zero corresponding to ground-state atomic ion limits.

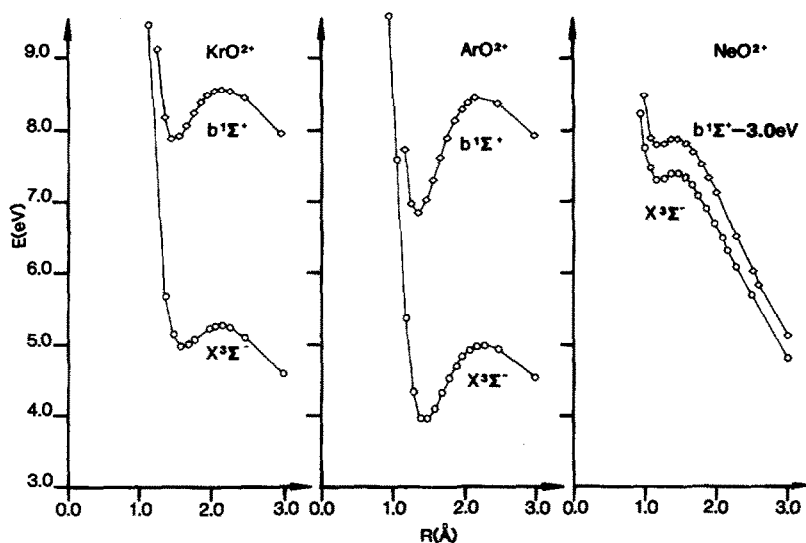


Fig. 5 Approximate potential curves for dications of rare-gas oxides, calculated using the procedure due to Hurley. Energy zero corresponds to ground-state atomic ion limits.

curves, with the experimental results presented in table 2, suggests that the large values (8–9 eV) for translational energy release observed to characterise unimolecular dissociation of  $\text{KrO}^{2+}$  and of  $\text{ArO}^{2+}$ , must correspond to dissociation of the  $b^1\Sigma^+$  states to ground-state atomic fragments. This can arise only if the delayed (microsecond) dissociation proceeds by a spin-forbidden curve-crossing to a repulsive triplet state of appropriate space symmetry. The very shallow potential wells predicted for  $\text{NeO}^{2+}$  could account for the absence of any experimental evidence for this species (tables 1 and 2).

One further correlation of the present experimental results can be attempted, though it is not applicable to the oxides if the above conjecture as to the predissociation mechanism is valid. Fig. 6 summarises the appropriate relationships. It is assumed, as discussed above, that the monocations  $\text{AY}^+$  which survive the few microseconds to the collision cell of the mass spectrometer are in electronic states correlating with  $\text{A}^+ + \text{Y}$ . It is further assumed that ionization energies of  $\text{AY}^+$ , determined in the charge-stripping experiments (table 1), correspond to 0–0 transitions for  $\text{AY}^+ \rightarrow \text{AY}^{2+}$ . Finally, the delayed unimolecular dissocia-

tions of  $\text{AY}^{2+}$  (table 2) are assumed to correspond to tunnelling through the barrier near its maximum. Under all of these assumptions, fig. 6

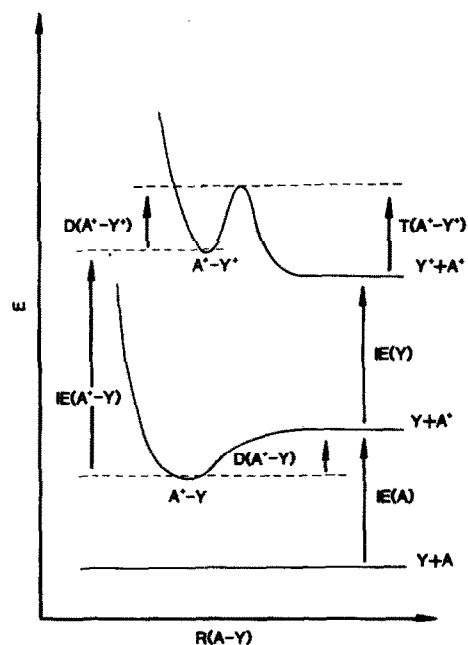


Fig. 6. Highly simplified energy diagram relating  $\text{A}^+ \text{Y}$  and  $\text{AY}^{2+}$  species (see text).

shows that the following relationship is valid

$$D(A^+-Y) - D(A^+-Y^+) \\ = IE(A^+Y) - IE(Y) - T(A^+-Y^+),$$

where  $D$  represents a dissociation energy,  $IE(A^+Y)$  is the charge-stripping value for the ionization energy, and  $T(Y^+-A^+)$  is the kinetic energy release accompanying unimolecular dissociation of  $AY^{2+}$ . If the oxides are excluded, as discussed above the following differences in dissociation energies can be deduced from the experimental data summarised in tables 1 and 2:

$$D(Xe^+-C) - D(Xe^+-C^+) = -3.7 \text{ eV},$$

$$D(Xe^+-N) - D(Xe^+-N^+) = 0.5 \text{ eV},$$

$$D(Kr^+-N) - D(Kr^+-N^+) = 1.1 \text{ eV}.$$

The uncertainties are probably as high as  $\pm 2$  eV in each case. The fact that  $XeC^{2+}$  is thus predicted to have a significantly deeper potential well than  $XeC^+$  is a direct consequence of the rather low charge-stripping energy (table 1), which was commented on above. This tentative conclusion is at least consistent in a qualitative sense with the deep potential wells for these  $AC^{2+}$  species predicted by Hurley's method [2,3] (fig. 3). No conclusion is possible for the two nitrides.

The need for reliable potential curves, of ground and excited states of these  $YA^{2+}$  species, is emphasised by the tentative nature of the present discussion. Extension of the ab initio molecular orbital calculations, reported previously [20] for diatomic dications comprised of first-row elements only, will be difficult.

### Acknowledgement

This work was supported by the Royal Society, by University College of Swansea and by NSERC (Canada).

### References

- [1] D.L. Cooper and S. Wilson, *Mol. Phys.* 44 (1981) 161.
- [2] A.C. Hurley and V.W. Maslen, *J. Chem. Phys.* 34 (1961) 1919.
- [3] A.C. Hurely, *J. Mol. Spectry.* 9 (1962) 18.
- [4] P. Jonathan, A.G. Brenton, J.H. Beynon and R.K. Boyd, *Intern. J. Mass Spectrom. Ion Phys.*, to be published.
- [5] R. Johnsen and M.A. Biondi, *Phys. Rev. A* 20 (1979) 87.
- [6] H. Helm, K. Stephan, T.D. Mark and D.L. Huestis, *J. Chem. Phys.* 74 (1981) 3844.
- [7] K. Stephan, T.D. Mark and H. Helm, *Phys. Rev. A* 26 (1982) 2981.
- [8] M. Guilhaus, A.G. Brenton, J.H. Beynon, M. Rabrenović and P. von R. Schleyer, *J. Phys. B* 17 (1984) L605.
- [9] F.H. Field and J.L. Franklin, *J. Am. Chem. Soc.* 83 (1961) 4509.
- [10] F.H. Field, H.N. Head and J.L. Franklin, *J. Am. Chem. Soc.* 84 (1962) 1118.
- [11] M.S.B. Munson, F.H. Field and J.L. Franklin, *J. Chem. Phys.* 37 (1962) 1790.
- [12] M.S.B. Munson, J.L. Franklin and F.H. Field, *J. Phys. Chem.* 67 (1963) 1542.
- [13] R.P. Morgan, J.H. Beynon, R.H. Bateman and B.N. Green, *Intern. J. Mass Spectrom. Ion Phys.* 28 (1978) 171.
- [14] M. Rabrenović, A.G. Brenton and J.H. Beynon, *Intern. J. Mass Spectrom. Ion Phys.* 52 (1983) 175.
- [15] M. Guilhaus, R.K. Boyd, A.G. Brenton and J.H. Beynon, *Intern. J. Mass Spectrom. Ion Phys.* 67 (1985) 209.
- [16] P.D. Bolton, G.W. Trott, R.P. Morgan, A.G. Brenton and J.H. Beynon, *Intern. J. Mass Spectrom. Ion Phys.* 29 (1979) 179.
- [17] T. Ast, C.J. Porter, C.J. Proctor and J.H. Beynon, *Bull. Soc. Chim. Beograd* 46 (1981) 135.
- [18] R.G. Cooks, J.H. Beynon, R.M. Caprioli and G.R. Lester, *Metastable ions* (Elsevier, Amsterdam, 1973).
- [19] M.H.R. Hutchinson, *Appl. Phys.* 21 (1980) 95.
- [20] R.W. Wetmore, R.J. LeRoy and R.K. Boyd, *J. Phys. Chem.* 88 (1984) 6318.
- [21] K.P. Huber and G. Herzberg, *Spectroscopic constants of diatomic molecules* (Van Nostrand, Princeton, 1979).
- [22] C.E. Moore, *Atomic energy levels as derived from the analyses of optical spectra*, NSRDS-NBS 35 (1971).